

The Transition from Vesicles to Micelles Induced by Octane in Aqueous Surfactant Two-Phase Systems

Min Mao, Jianbin Huang,* Buyao Zhu, and Jianping Ye

Institute of Physical Chemistry, Peking University, Beijing 100871, P.R. China

Received: February 26, 2001; In Final Form: July 18, 2001

The transition from vesicles to micelles by adding octane into the dodecyl-pyridinium chloride (DPCI)/sodium laurate (SL), and dodecyltrimethylammonium bromide (DTAB)/SL aqueous two-phase systems has been studied. The two-phase systems were transformed into single-phase isotropic solutions with the addition of a certain amount of octane. The results of dynamic light scattering (DLS) demonstrate the decrease of large aggregates (vesicles) and the increase of the small aggregates (spherical micelles) upon octane addition. Such transformation of the surfactant aggregates was also corroborated by the results of time-resolved fluorescence quenching (TRFQ) and viscometry. The change of the phase behavior was discussed on the basis of the interaggregate interactions influenced by the variation of organized assemblies.

Introduction

Various kinds of organized assemblies, such as vesicles, micelles, etc., and the peculiar phase behavior in mixed cationic and anionic surfactant systems have attracted great attention in the past decade.^{1–6} In some catanionic mixtures, a novel phenomenon is the coexistence of two dilute aqueous surfactant phases (ASTP), which would have applications in the partitioning and analysis of biomaterials.⁵ According to the main form of organized assemblies in mixed systems, ASTP can be divided into two categories. One is induced by the entanglement of rod-like micelles,^{3,5} and the other is composed of vesicles which packed densely and sparsely in the upper and bottom phase, respectively.⁷ Compared with the former that was under more investigation, the mechanism of the latter is still not clear. However, the interactions between the vesicles should play a key role in this case.

It is well known that the structure transformation of surfactant aggregates surely induces the change of interaggregate interactions.⁸ The extensive research on the transitions between micelles and vesicles in catanionic mixtures has been investigated by various techniques.^{9–15} However, in contrast to the numerous works on the aggregate transformation induced by the addition of salts and the variation of mixing ratio or surfactant concentration, the effects of hydrocarbon addition on the aggregate transformation in catanionic mixtures are less studied.¹⁶

In this work we present a study on the organized microstructures and the subsequent change of the phase behavior in the second kind of ASTP upon the solubilization of hydrocarbons. In two catanionic surfactant systems, freeze-fracture electron microscopy (FF-TEM), dynamic light scattering (DLS), time-resolved fluorescence quenching (TRFQ), and viscometry were used to characterize the formation and transformation of microstructures in ASTP with different octane concentration. A new phenomenon was found that catanionic vesicles could be transformed into rod-like micelles and eventually to spherical micelles by octane addition, which would shed some light on the mechanism of this peculiar kind of phase separation and be important to open a vista of the practical uses of ASTP.

Experimental Section

Materials. Sodium laurate (SL) and sodium 10-undecanoate (UNDA) were prepared by neutralizing the corresponding carboxylic acid with NaOH in ethanol, then the solvent was removed and sodium alkylcarboxylates were vacuum dried. Lauric acid was recrystallized five times from an ethanol–water mixture. 10-Undecanoate was recrystallized three times from ethanol. Sodium dodecylbenzenesulfonate (SDBS) was used as received from Acros. Decyltrimethylammonium bromide (DeTAB), dodecyltrimethylammonium bromide (DTAB), and dodecyl-pyridinium chloride (DPCI) were synthesized from *n*-alkyl bromide and trimethylamine or pyridine. The crude products were recrystallized five times from the mixed solvents of ethanol–acetone or ether–acetone. The purity of all the surfactants was examined and no surface tension minimum was found in the surface tension curve. Pyrene obtained from Sigma and dibutylaniline (DBA) obtained from Aldrich were used as received. The other reagents were products of Beijing Chemical Co., A. R. grade.

Methods. Sample Preparation. The aqueous two-phase systems were prepared by weighing cationic surfactant and water first into the sample vial (allowing the cationic surfactant to dissolve), and then adding anionic surfactant stock solution of desired concentration. After sealing, samples were vortex mixed and then equilibrated in a thermostated bath controlled to 30 °C. The formation of DPCI/SL aqueous two-phase system usually takes several hours, and the formation of DTAB/SL aqueous two-phase system would take more time, about twenty hours. The prepared samples were stable even after one year. The desired amount of octane was added to the samples using a syringe. The sealed samples were equilibrated in a thermostatic bath for at least one month before investigations.

Electron Microscopy. Samples for electron microscopy were prepared by freeze-fracture replication according to standard techniques. Fracturing and replication were carried out in a high vacuum freeze-etching system (Balzers BAF-400D). Replicas were examined in a JEM-100CX electron microscope.

Dynamic Light Scattering (DLS). Dynamic light scattering measurements were made using a spectrometer of standard design (ALV-5000/E/WIN Multiple Tau Digital Correlator) and a Spectra-Physics 2017 200 mW Ar laser (514.5 nm wavelength). The scattering angle was of 90°, and the intensity

* Corresponding author. E-mail: jbhuan@chem.pku.edu.cn. Fax: 8610-62751708. Tel.: 8610-62753557.

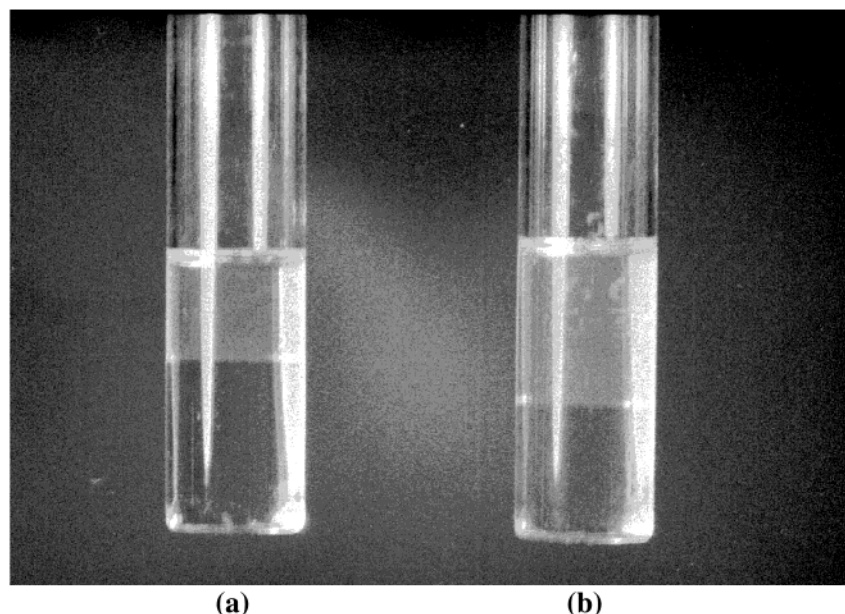


Figure 1. Photographs of the aqueous surfactant two-phase systems (ASTP) (a) DTAB/SL (1.4:1, $C_{\text{total}} = 0.08$ M); (b) DPCI/SL (1.3:1, $C_{\text{total}} = 0.1$ M).

autocorrelation functions were analyzed using the methods of Cumulant and Contin. The solutions were centrifuged at a speed of 12000 rpm/min for 30 min to remove the dust before the experiment. The experimental temperature was controlled to 30 °C.

Time-Resolved Fluorescence Quenching (TRFQ). Pyrene was added to the surfactant solutions by the following method. The appropriate amount of pyrene/ethanol stock solution was added to a flask. Ethanol was evaporated by letting nitrogen gas gently flow over the solution. Then the desired amount of surfactant solution was added to the flask and was stirred overnight. The concentration of pyrene was kept low (1×10^{-5} M) to prevent excimer formation. The quencher dibutylaniline (DBA) in ethanol was added to the surfactant solution directly (the amount of ethanol in each sample < 1 vol %; usually the effect of ethanol at this concentration on the surfactant aggregates is insignificant^{9,10}). All of the solutions were degassed by high-pure nitrogen for 15 min before measurements to eliminate the effect of oxygen.

Time-resolved fluorescence decay of pyrene was performed on a Horiba NAES 1100 nanosecond fluorometer. The excitation wavelength was 337 nm and the emission was collected at 400 nm. The fluorescence decays of pyrene were fitted according to eq 1 by using DECAN 1.0 software. The χ^2 of these fittings were from 0.978 to 1.607.

Viscometry. Viscosity measurements were performed on a low-shear 30 rheoanalyzer. All samples equilibrated for 30 min before any measurement. Each result was the average of five runs. The temperature was controlled to 30 ± 0.1 °C during the experiment.

Results and Discussion

Formation and Microstructures in the Aqueous Surfactant Two-phase Systems. The phenomena of surfactant aqueous two-phase systems were observed at DPCI/SL mixed system (molar ratio 1.3:1, $C_{\text{total}} = 0.1$ M) and DTAB/SL system (molar ratio 1.4:1, $C_{\text{total}} = 0.08$ M). The interface between the two transparent phases is clear (Figure 1) and the volume ratio of the upper and bottom phases is very sensitive to the mixing ratio. It is common that the L_{α} phase can separate from the

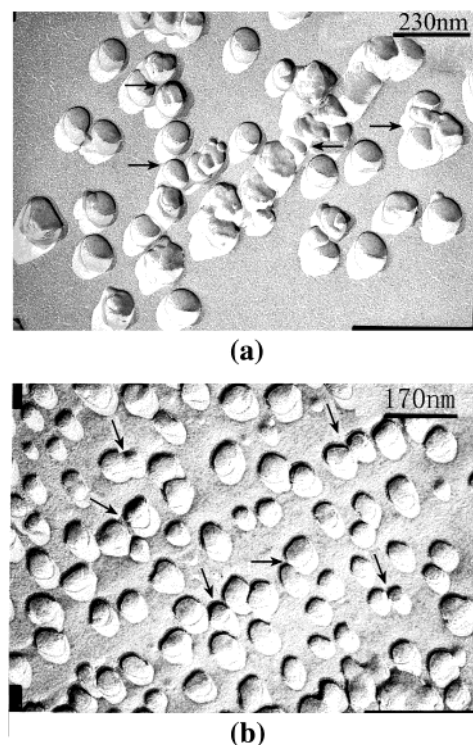


Figure 2. FF-TEM micrographs of upper phases in (a) DPCI/SL ASTP; (b) DTAB/SL ASTP. Vesicle-vesicle aggregation is clearly shown (see the arrows).

bulk solution;⁶ however, the two phases in these systems studied were not birefringent, indicating no typical L_{α} texture formation. In fact, similar phase separation phenomena were also observed in many mixtures of cationic surfactants and sodium alkylcarboxylates. TEM observation demonstrated that these mixed systems were of the second kind of ASTP. Figure 2 clearly shows the vesicle formation in the upper phase. However, vesicles may not be the only existing organized assemblies since it is difficult to determine the existence of micelles by FF-TEM.

Dynamic light scattering can be used to measure the translational diffusion coefficient $D(= \Gamma/q^2$, with q being the

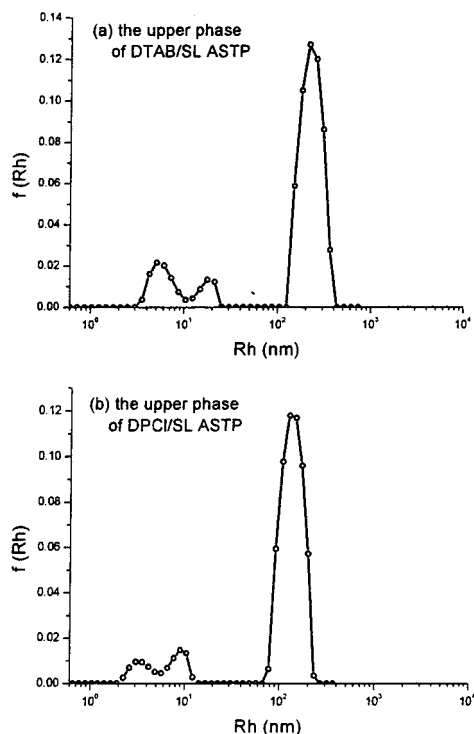


Figure 3. The hydrodynamic radius (R_h) distribution of the surfactant aggregates in the upper phases of (a) the DTAB/SL ASTP; (b) the DPCI/SL ASTP.

TABLE 1: The Polydispersity Index (PI) of the Upper Phases

system	DTAB/SL	DPCI/SL
PI	0.444	0.416

magnitude of the momentum transfer vector and the Γ the characteristic line width). With the Stokes–Einstein relation

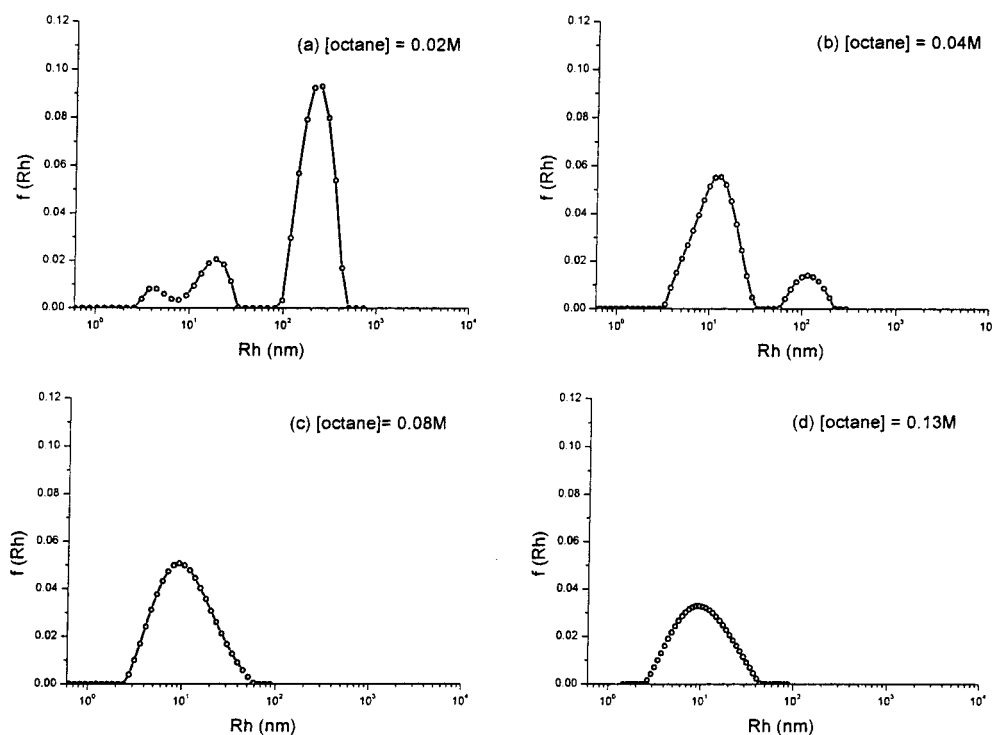


Figure 4. The hydrodynamic radius (R_h) distributions of the surfactant aggregates in the DPCI/SL ASTP upon the solubilization of octane. (a) [octane] = 0.02 M; (b) [octane] = 0.04 M; (c) [octane] = 0.08 M; (d) [octane] = 0.13 M.

$$R_h = k_B T / 6\pi\eta D$$

we can determine the equivalent hydrodynamic radius R_h . CONTIN analysis of the field correlation function $g^{(1)}(\tau)$, with $g^{(1)}(\tau) = \int G(\Gamma) e^{-\Gamma\tau} d\Gamma$, yields the normalized characteristic line width distribution function $G(\Gamma)$, where $\Gamma G(\Gamma)$ is defined as the intensity distribution function is proportional to the scattered intensity with R_h in the logarithmic scale. Figure 3 shows the hydrodynamic radius R_h distribution of the surfactant aggregates in the upper phases of ASTP. As the polydispersity is an inherent feature of mixed cationic and anionic surfactant systems, the polydispersity index (PI) of the upper phases is also fairly large (Table 1). CONTIN analysis (Figure 3) shows that there are various kinds of the surfactant aggregates coexisting in the upper phases of ASTP. Combining the results of FF-TEM, there are still micelles coexisting with vesicles in the upper phases of ASTP. The size discrepancies of the vesicles between the result of EM and DLS may be attributed to the aggregation of vesicles in the upper phases of the two systems (as showed in the Figure 2). Since DLS would take the aggregated vesicles as a single particle, the equivalent hydrodynamic radius of vesicles from DLS would be much larger than that EM would show.

Phase Behavior and the Organized Microstructure Transition in Mixed Cationic–Anionic Surfactant Systems with Octane Addition. *A. Phase Behavior.* When hydrophobic molecules are solubilized in surfactant aggregates, the balance of various intra-aggregate interactions will be influenced, thus the shape and size of the aggregates are also changed. The structure transitions of surfactant aggregates upon the solubilization of hydrocarbons have been investigated extensively using many experimental techniques in the micellar systems.^{17–20} However, there were only a few investigations on the morphology change of vesicles upon the addition of aliphatic hydrocarbons.^{16,21}

In DPCI/SL aqueous two-phase systems, the volume of the upper phase decreased with the increase of the octane concen-

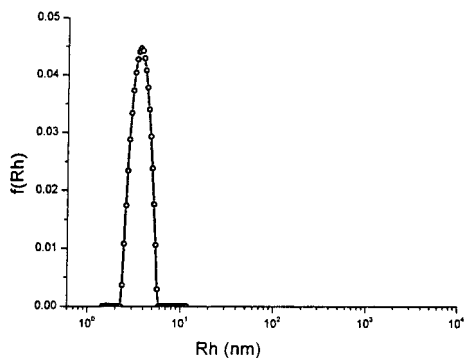


Figure 5. The hydrodynamic radius (R_h) distribution of the surfactant aggregates in the DeTAB/UNDA ASTP upon the solubilization of 0.09 M octane.

tration. When the concentration of octane increased to 0.02 M, the interface between the two phases gradually became indistinct and disappeared after two weeks. The maximum octane concentration in this study was 0.13 M, above which it was very difficult to dissolve the octane. A similar phenomenon was also observed in DTAB/SL ASTP system.

The effect of octane on the upper phase is more obvious than that on the bottom phase in ASTP, since surfactants are usually rich in the upper phase and poor in the bottom phase.^{5,23} In the DTAB/SL aqueous two-phase system, the upper phase was separated to investigate the structure transition of surfactant aggregates with the solubilization of octane. It was interesting to find that the upper phase separated into two phases again when the octane concentration is below 0.02 M. However, the upper phase transformed back into an isotropic solution when the concentration of octane increasing to 0.02 M. Mixing such isotropic solution with the original bottom phase, no phase separation was observed but a homogeneous solution was obtained. All the above results draw the conclusion: the disappearance of the phase separation is mainly due to the change of surfactant aggregates in the upper phase.

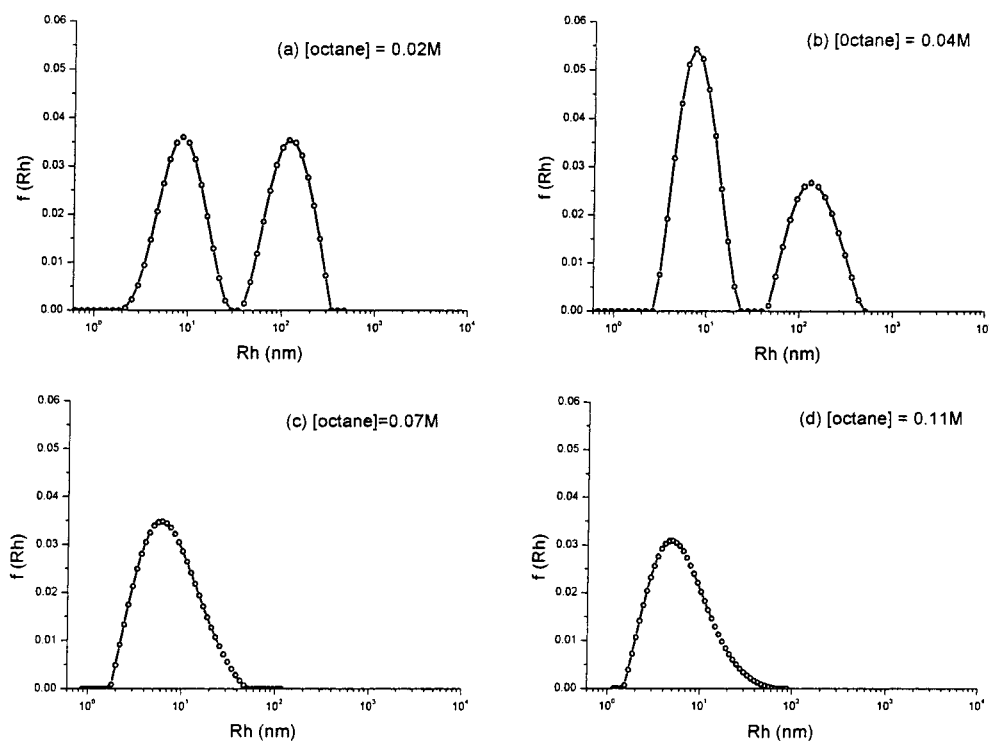


Figure 7. The hydrodynamic radius (R_h) distribution of the surfactant aggregates in the upper phase of the DTAB/SL ASTP upon the solubilization of octane. (a) [octane] = 0.02 M; (b) [octane] = 0.04 M; (c) [octane] = 0.07 M; (d) [octane] = 0.11 M.

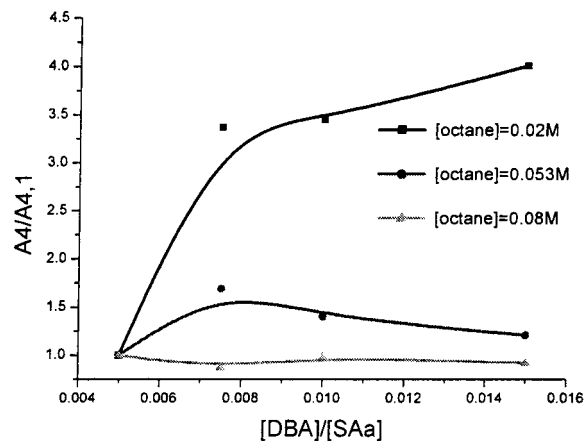


Figure 6. The variation of A_4 as a function of quencher concentration for different octane concentration.

B. Structure Transition of the Surfactant Aggregates in Solution. The disappearance of the phase separation can be attributed to the structure change of the surfactant aggregates in solution. Figure 4 shows the hydrodynamic radius R_h distribution of surfactant aggregates in DPCI/SL ASTP system upon the addition of octane. The size distribution of surfactant aggregates at different octane concentration is shown in four separate panels. At a low octane concentration (0.02 M), a number of vesicles still exist (Figure 4a). With the octane concentration increasing to 0.04 M, the number of vesicles decreases drastically (Figure 4b). When the octane concentration reaching 0.08 M or more, the vesicles almost disappear in the system (Figure 4c,d). These clearly show that the number of vesicles gradually decreases with the increase of octane concentration. Finally the micelles become the predominant aggregates in the solution when the octane concentration approaches the maximum. The similar transition from vesicles to micelles was also observed in DTAB/SL ASTP system. The transition from vesicles to micelles was more obvious in

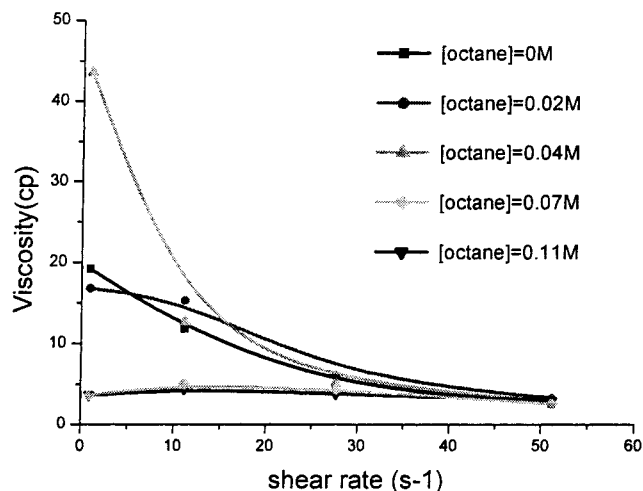


Figure 8. The viscosity of the upper phase of DTAB/SL ASTP at different octane concentration.

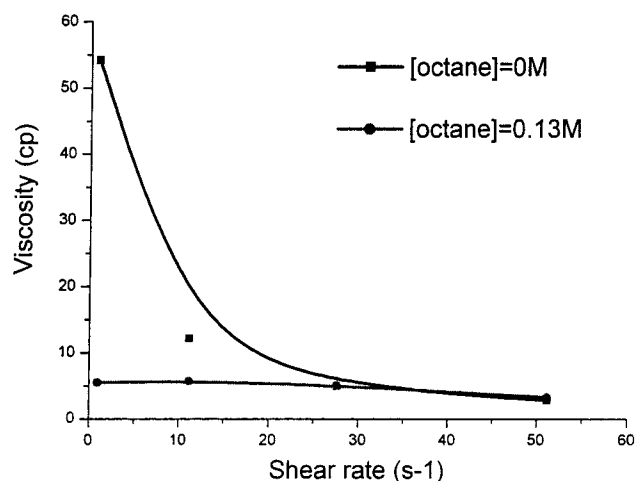


Figure 9. The viscosity of the DPCI/SL ASTP at different octane concentration.

DeTAB/UNDA (molar ratio of 1:1, $C_{\text{total}} = 0.13 \text{ M}$) aqueous two-phase system, in which vesicles also existed in both phases. When solubilized octane reaches 0.09 M in the whole system, this ASTP system turns to be a narrow-dispersed micellar solution ($PI = 0.044$, $R = 3.5 \text{ nm}$) (see Figure 5).

The results of TRFQ also confirm the process of transition from vesicles to micelles by octane addition. The time dependent fluorescence intensity of a probe in the micelle at the presence of a quencher is thought to obey the following Infelta–Tachiya equation:²⁴

$$I(t) = I(0) \exp[-A_2 t - A_3 (1 - \exp(-A_4 t))] \quad (1)$$

where I_0 is the intensity of fluorescence at $t = 0$, A_2 is the fluorescence decay rate constant of the probe without quencher, and A_4 is the quenching rate constant of the probe by a quencher in the micelle. A_2 and A_4 are independent of quencher concentration. A_3 represents the average number of quenchers per micelle. Assuming a monodispersed micelle solution, the micelle aggregation number N can be obtained from

$$N = (C - \text{cmc}) A_3 / [Q] \quad (2)$$

where C is the concentration of the surfactant and $[Q]$ is the concentration of quencher. From eq 1, the fluorescence decay curves of micelle solution appear to be of a double-exponential form.

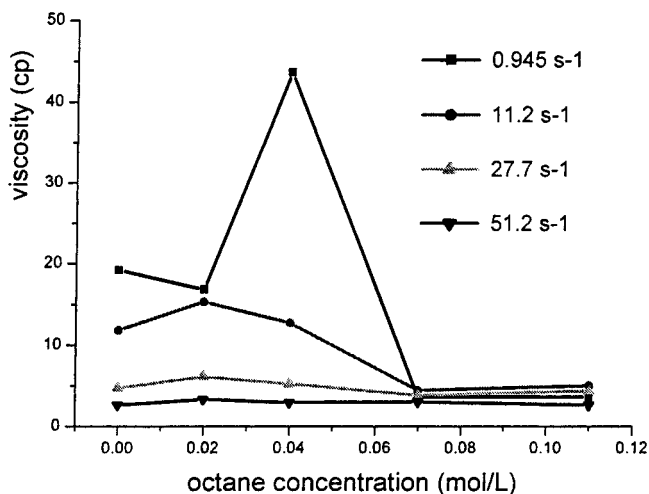


Figure 10. The viscosity of the upper phase of DTAB/SL ASTP at different shear rates.

In vesicles and other large aggregates, the time dependent fluorescence intensity of a probe at the presence of a quencher is thought to obey the modified Stern–Volmer equation:²⁵

$$I(t) = I(0) \exp(-A_5 t - A_6 t^{1/2}) \quad (3)$$

A_5 and A_6 both depend on quencher concentration. Thus the decay curves of samples containing large aggregates appear in a monoexponential form. If micelles and vesicles coexist in the solution, the fluorescence decay curves obey a linear combination of eqs 1 and 3. If the curves are forced to fit the form of eq 1, A_4 shows the dependence on quencher concentration and the ratio of vesicles to micelles.¹⁰ The experimental data gradually departs from eq 1 when the ratio of vesicles to micelles increases. At very high ratio of vesicles to micelles, the data do not obey eq 1, and eq 3 should be used. Hence, TRFQ can be used to track the transition between the vesicles and micelles.

In the DTAB/SL system, TRFQ data were measured for the solutions with octane concentrations of 0.02, 0.053 and 0.08 M. For all the samples, the slope of the fluorescence decay at long time is independent of the quencher concentration and equal to the slope of the unquenched decay, indicating the presence of micelles in all systems. This also agrees with the result of DLS. With the increase of octane concentration, the quality of the fit to eq 1 increases. The variation of A_4 (obtained by fitting the data according to eq 1) with the concentration of quencher has been found to be diagnostic for vesicles: the more positive the slope of A_4 vs quencher concentration, the more vesicles in the solution. In the DTAB/SL system, the slope of A_4 vs quencher concentration decreases with the increase of octane concentration (Figure 6), indicating the decrease of the vesicle population. At the octane concentration of 0.08 M, the fluorescence decay shows the typical form of the micelle solution since A_4 is independent of quencher concentration. The micelle aggregation number, calculated from eq 2 assuming the monodispersion of micelles, is about 205.

The DLS results in Figure 7 also demonstrated the same tendency of structure transition of surfactant aggregates. When the octane concentration increases to 0.11 M, micelles become the predominant surfactant aggregates in the solution.

The transition from vesicles to micelles was also supported by the results of viscosity. Figure 8 shows the viscosity of the upper phase of DTAB/SL ASTP system as a function of shear rate at different octane concentration. Stirring the solution with a rotating shaft, we did not observe the Weissenberg effect,

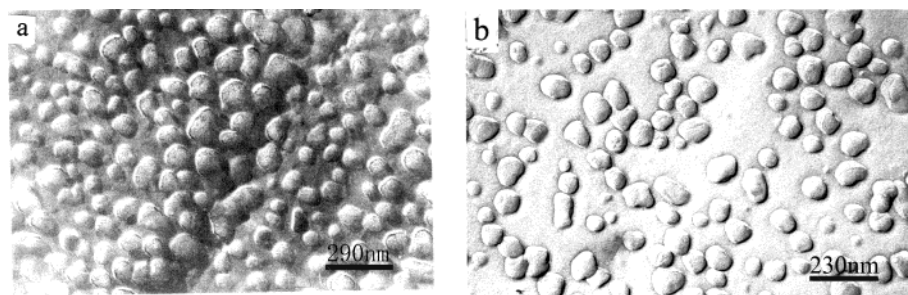


Figure 11. FF-TEM micrographs of the mixed DTAB/SDBS (mixing ratio 2.5:1, $C_{\text{total}} = 0.028$ M) solution. (a) without the addition of octane; (b) [octane] = 0.053 M.

which is common to a viscoelastic liquid. When the octane concentration is lower than 0.04 M, the viscosity decreases as the shear rate increases. However, when the octane concentration increases to 0.07 M or more, the viscosity of solutions is independent of the shear rate. An analogous result is also observed in the DPCI/SL ASTP system (Figure 9). The transition of organized assemblies in this system is very obvious in the curves of viscosity vs octane concentration at different shear rates (Figure 10). It is noteworthy that the viscosity increases and then decreases drastically with the addition of octane at low shear rates. For example, at the shear rate of 0.945 s^{-1} , the viscosity of the solution is 19.2, 46.2, and 3.6 cP when the octane concentration is 0, 0.04, and 0.07 M, respectively. Such a large viscosity change should be accredited to the variation of organized assemblies. The increase of the viscosity may be due to the increase of rod-like micelles, showing the transition from vesicles to rod-like micelles. As far as the decrease of viscosity, it can be assumed that the solubilization of aliphatic hydrocarbons would transform rod-like micelles into spherical ones and reduce the viscosity of the solution.

However, the transition from vesicles to micelles upon the solubilization of octane was not observed in the mixed SDBS/DTAB (mixing ratio 1:2.5, $C_{\text{total}} = 0.028$ M) solution, which was thought to be “pure” catanionic vesicle solution¹⁰ (containing only vesicles). After addition of 0.053 M octane, the vesicles still existed, instead of transforming into micelles (Figure 11). The reason for the different microstructure transition between the SDBS/DTAB and SL/DTAB systems with octane addition is still not clear and needs further investigation.

C. The Mechanism for Formation and Variation of Cationic–Anionic ASTP. There are four main types of interactions between the surfactant aggregates: electrostatic interaction, van der Waals force, steric force, and hydration force.⁸ The interplay between the former two forces forms the basis of DLVO theory. The latter two kinds of forces are short range compared with the former two forces. According to DLVO theory, the minimum energy point (the secondary minimum) may be attained at the balance of repulsive electrostatic interaction and the attractive van der Waals force. Aggregation (generally called flocculation) in the secondary minimum is not very stable due to the shallow energy well. The presence of electrolyte or the increase of the particle size can enhance such flocculation.²⁶

The phase behavior of surfactant solutions is closely related to the surfactant aggregates in the solution and the interactions between them. The phase separation in mixed cationic and anionic surfactant solutions containing vesicles may be accredited to the difference in the interactions between surfactant aggregates in the upper and bottom phase. The mixing ratio of surfactants in ASTP is close to equimolarity and the composition of vesicles is closer to equimolarity than the phase composition,²⁷ the surface potential ψ_0 of vesicles is low, and the double-

TABLE 2: Phase Compositions of the Two Phases in the DPCI/ASTP System

	$C_{\text{SPCI}} (\text{mol/L}) \times 10^3$	$C_{\text{SL}} (\text{mol/L}) \times 10^3$	molar ratio
upper phase	92.2	89.9	1.026
bottom phase	3.85	1.44	2.67

layer repulsion is very weak in these systems. The two phases of the DPCI/SL ASTP system were separated to determine their compositions (Table 2).²³ It is showed that the surfactant ratio of the upper phase is closer to equimolarity, which makes it possible for the vesicles to flocculate. The flocculated vesicles in the upper phases of DPCI/SL and DTAB/SL ASTP system are clearly showed in Figure 2 (see the arrows). In fact, the aggregation of vesicles due to the electrolyte addition was also observed in mixed cetyltrimethylammonium bromide/dodecylbenzene sulfuric acid solution.²⁸ When enough vesicles (weakly charged) become flocculated, they will separate from the solution to form the upper phase while the more charged vesicles remain dispersed in the bottom phase. Thus the composition of the upper phase is more close to equimolarity than that of the bottom phase.

Upon the solubilization of octane, the vesicles transform into spherical micelles. Since the van der Waals forces decrease with the decrease in the particle size, the total interaction between the surfactant aggregates becomes repulsive and the secondary minimum disappears. Hence the interactions between the surfactant aggregates in the upper phase are similar to those in the bottom phase. Consequently, the phase separation cannot be maintained and the two-phase systems transform back into homogeneous solution.

Conclusion

Transformation of organized assemblies by adding octane into the two cationic and anionic surfactant mixed systems was systematically studied. The solubilization of octane into the aqueous surfactant two-phase systems induces the gradual transition from vesicles to micelles. The results of DLS, TRFQ, and viscometry demonstrate the decrease of vesicles and the increase of micelles upon octane addition. The transition from vesicles to micelles changes the interactions between the surfactant aggregates in the upper phase, which leads to the two-phase systems transforming into single-phase isotropic solutions.

Acknowledgment. This work was supported by National Natural Science Foundation (29733110 and 29992590-4) and the doctoral program of higher education of China.

References and Notes

- (1) Marques, E.; Khan, A.; da Graca Miguel, M.; Lindman, B. *J. Phys. Chem.* **1993**, *97*, 4729.

- (2) Huang, J.-B.; Zhao, G.-X. *Colloid Polym. Sci.* **1995**, 273, 156.
- (3) Yacilla, M. T.; Herrington, K. L.; Brasher, L. L.; Kaler, E. W. *J. Phys. Chem.* **1996**, 100, 5874.
- (4) Koehler, R. D.; Raghavan, S. R.; Kaler, E. W. *J. Phys. Chem. B* **2000**, 104, 11035.
- (5) Zhao, G.-X.; Xiao, J.-X. *J. Colloid Interface Sci.* **1996**, 177, 513.
- (6) Klaus, H.; Hoffmann, H.; Jingchen, H. *J. Phys. Chem. B* **2000**, 104, 2781.
- (7) Zhao, G.-X.; Yu, W.-L.; Gong, Y.-J.; Zhu, B.-Y. *Chinese Chem. Lett.* **1998**, 9, 1059.
- (8) Israelachvili, J. N. *Intermolecular and Surface Forces*; Academic Press: New York, 1992.
- (9) Herrington, K. L.; Kaler, E. W.; Miller, D. D.; Zasadzinski, J. A. N.; Chiruvolu, S. *J. Phys. Chem.* **1993**, 97, 13792.
- (10) Sonderman, O.; Herrington, K. L.; Kaler, E. W.; Miller, D. D. *Langmuir* **1997**, 13, 5531.
- (11) Bergstrom, M.; Pedersen, J. S.; Schurtenberger, P.; Egelhaaf, S. U. *J. Phys. Chem. B* **1999**, 103, 9888.
- (12) Villeneuve, M.; Kaneshina, S.; Imae, T.; Aratono, M. *Langmuir* **1999**, 15, 2529.
- (13) O'Connor A.; Hatton, T. A.; Bose, A. *Langmuir* **1997**, 13, 6931.
- (14) Brasher, L. L.; Herrington, K. L.; Kaler, E. W. *Langmuir* **1995**, 11, 4267.
- (15) Salkar, R. A.; Mukesh, D.; Samant, S. D.; Manohar, C. *Langmuir* **1998**, 14, 3778.
- (16) Gradzielski, M.; Hoffmann, H.; Langevin D. *J. Phys. Chem.* **1995**, 99, 12612.
- (17) Tornblom, M.; Henriksson, U. *J. Phys. Chem. B* **1997**, 101, 6028.
- (18) Hoffmann, H.; Ulbricht, W. *J. Colloid Interface Sci.* **1989**, 129, 388.
- (19) Bayer, O.; Hoffmann, H.; Ulbricht, W.; Thurn, H. *Adv. Colloid Interface Sci.* **1986**, 26, 177.
- (20) Christian, S. D., Scamehorn, F. F., Eds.; *Solubilization in Surfactant Aggregates*; Marcel Dekker: New York, 1995.
- (21) Chaieb, S.; Rica, S. *Phys. Rev. E* **1998**, 58, 7733.
- (22) Champion, J. T.; Gilkey, J. C.; Lamparski, H.; Retterer, J.; Miller, R. M. *J. Colloid Interface Sci.* **1995**, 170, 569.
- (23) Zhu, B.-Y.; Zhang, P.; Huang, J.-B.; Zhao, G.-X. *Acta Physico-Chim. Sinica* **1999**, 15, 110.
- (24) Gehlen, M. H.; De Schryver, F. C. *Chem. Rev.* **1993**, 93, 199.
- (25) (a) Almgren, M. *Adv. Colloid Interface Sci.* **1992**, 41, 1. (b) Miller, D. D.; Evans, D. F. *J. Phys. Chem.* **1989**, 93, 232. (c) Miller, D. D.; Magid, L. J.; Evans, D. F. *J. Phys. Chem.* **1990**, 94, 5921.
- (26) Ohki, S.; Ohshima, H. *Colloids Surf. B* **1999**, 14, 27.
- (27) Brasher, L. L.; Kaler, E. W. *Langmuir* **1996**, 12, 6270.
- (28) Yaacob, I. I.; Bose, A. *J. Colloid Interface Sci.* **1996**, 178, 638.